Rheologica Acta (2023) 62:433–445
https://doi.org/10.1007/s00397-023-01411-1

ORIGINAL CONTRIBUTION

Modeling elongational viscosity of polystyrene Pom-Pom/linear and Pom-Pom/star blends

Valerian Hirschberg[1] · Shan Lyu[1] · Max G. Schußmann[1] · Manfred Wilhelm[1] · Manfred H. Wagner[2]

Received: 26 May 2023 / Revised: 11 July 2023 / Accepted: 22 July 2023 / Published online: 3 August 2023

Abstract

The elongational rheology of blends of a polystyrene (PS) Pom-Pom with two linear polystyrenes was recently reported by Hirschberg et al. (J. Rheol. 2023, 67:403–415). The Pom-Pom PS280k-2x22-22k with a self-entangled backbone ($M_{w,bb}$ = 280 kg/mol) and 22 entangled sidearms ($M_{w,a}$ = 22 kg/mol) at each of the two branch points was blended at weight fractions from 75 to 2 wt% with two linear polystyrenes (PS) having M_w of 43 kg/mol (PS43k) and 90 kg/mol (PS90k), respectively. While the pure Pom-Pom shows strong strain hardening in elongational flow (SHF > 100), strain hardening (SHF > 10) is still observed in Pom-Pom/linear blends containing only 2 wt% of Pom-Pom. The elongational start-up viscosities of the blends with Pom-Pom weight fractions above 10 wt% are well described by the Molecular Stress Function (MSF) model, however, requiring two nonlinear fit parameters. Here we show that quantitative and parameter-free modeling of the elongational viscosity data is possible by the Hierarchical Multi-mode Molecular Stress Function (HMMSF) model based on the concepts of hierarchical relaxation and dynamic dilution. In addition, we investigated the elongational viscosity of a blend consisting of 20 wt% Pom-Pom PS280k-2x22-22k and 80 wt% of a PS star with 11 arms of $M_{w,a}$ = 25 kg/mol having a similar span molecular weight as PS43k and similar $M_{w,a}$ as the Pom-Pom. This work might open up possibilities toward polymer upcycling of less-defined polymers by adding a polymer with optimized topology to gain the intended strain hardening, e.g., for film blowing applications.

Keywords Pom-pom · Long-chain branching · Elongational viscosity · Strain hardening · Polymer blends · HMMSF model

Introduction

Strain hardening in elongational melt flow is a highly beneficial material property of polymers regarding their processability. Following the idea of the tube model, strain hardening in elongational flow is caused on the molecular level by chain stretching (Larson 1999). However, linear polymers show rather weak strain hardening at strain rates above the inverse of the Rouse relaxation time. This regime may be reached at rather low temperatures, but usually not at higher temperatures which are typical for polymer processing. However, strain hardening can also be induced on the molecular level by long-chain branching (Abbasi et al. 2017; Huang 2022; Lentzakis et al. 2013) with at least two branch points of the polymer molecule (McLeish and Larson 1998). The simplest topology fulfilling this requirement is the so-called Pom-Pom or the specific H-shaped topology where the H-topology has an arm number $q = 2$ at each end of the backbone (McKinley and Hassager 1999; McLeish et al. 1999; McLeish et al. 1999). Alternatively, blending of small amounts of ultrahigh molecular weight (UHMW) compounds into lower molecular weight grades also results in strain hardening provided the lower molecular weight component is well-entangled (Szántó et al. 2021; Tan et al. 2012; Wagner et al. 2005). In the second case, the strain hardening factors (SHF) are typically lower. Additionally, blending with UHMW polymer increases the zero-shear viscosity, whereas higher levels of branching usually result in lowering the viscosity. Blends of polymers with different

✉ Valerian Hirschberg
valerian.hirschberg@kit.edu

✉ Manfred H. Wagner
manfred.wagner@tu-berlin.de

[1] Institute of Chemical Technology and Polymer Chemistry (ITCP), Karlsruhe Institute of Technology (KIT), Engesserstraße 18, 76131 Karlsruhe, Germany

[2] Polymer Engineering/Polymer Physics, Berlin Institute of Technology (TU Berlin), Ernst-Reuter-Platz 1, 10587 Berlin, Germany

topology combine their rheological melt properties and allow tuning the desired processing properties.

Therefore, the so-called combinatorial rheology (Larson 2001), i.e., the combination of the rheological properties of different topologies, is of high interest from an experimental as well as a modeling point of view. Theoretical calculations of combinatorial rheology show a huge impact of the topology on the rheological properties of, e.g., blends of two polymers with different topologies. For example, using a hierarchical relaxation algorithm (Larson 2001), polybutadiene comb/linear and star/linear blends at the same molecular weight and at the same blend ratio were found to show significantly different zero-shear viscosities. Therefore, the validation of theoretical models by experimental evidence is of high interest to support model-driven development and optimization of molecular polymer topologies. This importance is also evident under the needs toward mechanical recycling of polymer melts.

However, so far, only a few well-defined model systems of blends with complex topology have been investigated experimentally (Ebrahimi et al. 2017; Hirschberg et al. 2023a; Lentzakis et al. 2019; Wagner et al. 2004). Blends of polyethylene (PE) are more often investigated, due to their high industrial relevance. For example, the blends of linear and branched polymers such as blends of linear low-density polyethylene (LLDPE) and low-density polyethylene (LDPE) (Ahirwal et al. 2014; Ajji et al. 2003; Wagner et al. 2005) and linear and branched polypropylene (Stange et al. 2005; Wagner et al. 2006) were studied and used to validate constitutive models. For one system of LDPE/LLDPE blends in elongational flow, similar maximal SHF = 10 was reported for the pure LDPE as well as for blends with only 20 wt% of LDPE and 80 wt% LLDPE by Wagner et al. (2004). They also showed that for LDPE/LLDPE blends with up to 90 wt% LLDPE, the Molecular Stress Function (MSF) model can very well describe the elongational behavior at Hencky strain rates above 0.1 s^{-1} by using the pure LPPE model parameters together with the linear viscoelastic relaxation spectrum of the respective blend.

Model polymer blends of low-disperse polymers with different molecular properties and topologies, e.g., two linear chains (López-Barrón et al. 2017; Nielsen et al. 2006; Shahid et al. 2019; Wagner et al. 2008) or linear chains blended with stars (Ebrahimi et al. 2017), H-shaped polymers (Ianniello and Costanzo 2022; Lentzakis et al. 2019), or Pom-Poms (Wagner et al. 2008), allowed the validation of constitutive models and molecular theories, such as the Extended Interchain Pressure (EIP) model (Wagner et al. 2021).

The elongational rheology of blends of a polystyrene Pom-Pom with two linear polystyrenes was presented by Hirschberg et al. (2023a). Pom-pom PS280k-2x22-22k with a self-entangled backbone ($M_{w,bb}$ = 280 kg/mol) and 22 entangled sidearms ($M_{w,a}$ = 22 kg/mol) at each of the two branch points was blended with two linear polystyrenes having molecular weights of 43 kg/mol (PS43k) and 90 kg/mol (PS90k), respectively. The full range of blends from 100 wt% of Pom-Pom down to only 2 wt% was investigated. In agreement with the analysis of the LLDPE/LDPE blends by Wagner et al. (2004), Hirschberg et al. (2023a) reported that the elongational rheology of blends with more than 10 wt% of Pom-Pom could be well described by the MSF model with two nonlinear fit parameters, β and f_{max}, and the respective linear viscoelastic relaxation spectrum of the blend. The parameter β was found to be independent of the molecular weight of the linear blend component, whereas f_{max} was lower for blends with PS90k than with PS43k.

Recently, Hirschberg et al. (2023b) showed that the elongational viscosity of 10 polystyrene Pom-Pom melts with backbone molecular weights $M_{w,b}$ of 100 to 400 kg/mol, arm molecular weights $M_{w,a}$ of 9 to 50 kg/mol, and 9 to 22 arms at each of the two branch points can be described quantitatively and parameter-free by the Hierarchical Multi-mode Molecular Stress Function (HMMSF) model, which is based on the concepts of hierarchical relaxation and dynamic dilution. Due to the high strain hardening of the Pom-Poms, brittle fracture is observed at higher strains and strain rates, which is well described by the entropic fracture criterion of Wagner et al. (2022). In extension of the work of Hirschberg et al. (2023b), the objective of this article is to demonstrate that a quantitative and parameter-free modeling of the elongational viscosity data of Pom-Pom/linear blends consisting of Pom-Pom PS280k-2x22-22k and linear PS43k as well as linear PS90k (Hirschberg et al. 2023a) by the HMMSF model is also possible. In addition, we investigated the elongational viscosity of a blend consisting of 20 wt% Pom-Pom PS280k-2x22-22k and 80 wt% of a PS star 11-25k with 11 arms of $M_{w,a}$ = 25 kg/mol having a similar span molecular weight as the PS43k and a similar $M_{w,a}$ as the Pom-Pom. As we will show in the following, the HMMSF can quantitatively describe the elongational behavior of the blends investigated, using as input parameters only the linear viscoelastic relaxation spectrum and the plateau modulus of the blend as determined from linear viscoelasticity.

Materials and experimental data

The linear polystyrenes were synthesized by living anionic polymerization. The Pom-Pom–shaped polystyrene was made by a combination of sequential living anionic polymerization and grafting onto as described in detail in Röpert et al. (2022a and 2022b). Within this synthetic route, monodisperse arms of PS anions are grafted onto a polyisoprene-*b*-polystyrene-*b*-polyisoprene (ISI) triblock copolymer. Where a low volume fraction of PI (typically 5

Table 1 Pom-pom/linear polystyrene blends with Pom-Pom 280k-2x22-22k and linear PS43k and 90k. $\varphi_{Pom-Pom}$ indicates the weight percent of Pom-Pom in the blends, G_N^0 is the plateau modulus, and η_0 is the zero-shear viscosity at $T = 160$ °C

Sample	Blends with PS43k		Blends with PS90k	
$\varphi_{Pom-Pom}$ (wt%)	G_N^0 (kPa)	η_0 (kPa s)	G_N^0 (kPa)	η_0 (kPa s)
100	240	833	240	833
75	230	231	180	240
50	280	97	190	130
20	130	10	140	58
10	220	6.6	180	58
5	290	5.5	230	55
2	310	4.0	130	29
0	-	3.0	-	25

Table 2 Pom-pom 280k-2x22-22k blended with PS star 11-25k. $\varphi_{Pom-Pom}$ indicates the weight percent of Pom-Pom in the blends, G_N^0 is the plateau modulus, and η_0 is the zero-shear viscosity at $T = 160$ °C

Sample	Blend with PS star 11-25k	
$\varphi_{Pom-Pom}$ (wt%)	G_N^0 (kPa)	η_0 (kPa s)
20	260	12
0	-	5.1

wt% at each side) is used as branching points at both ends of the polymer, the polyisoprene blocks are afterward functionalized via epoxidation, and the epoxy ring is opened via a defined polystyrene anion to achieve the controlled arm length. This synthetic route yields low-disperse Pom-Pom model systems.

The two linear PS have $M_w = 43$ kg/mol and 90 kg/mol and a dispersity of $Đ = 1.04$ and 1.05, respectively. The blends were made by a four-step solvent blending procedure similar to the one described in the literature (Shahid et al. 2019). First, linear and Pom-Pom PS were both dissolved in tetrahydrofuran (THF) at room temperature and stirred overnight, followed by slow evaporation and drying under vacuum for 24 h at 40 °C and a final 2 h drying under vacuum at 115 °C, slightly above the glass transition temperature (T_g) of PS to remove the last remaining traces of THF. A summary of the samples considered and their respective weight fraction $\varphi_{Pom-Pom}$ of Pom-Pom PS280k-2x22-22k is given in Tables 1 and 2.

Small amplitude oscillatory shear (SAOS) and uniaxial extensional measurements were conducted with an ARES-G2 rheometer (TA Instruments, Newcastle, USA) using a 13-mm plate-plate geometry for SAOS measurements as well as an extensional fixture (EVF) for uniaxial elongational tests. SAOS was measured between 130 and 220 °C, using a frequency range of $\omega = 0.1$–100 rad/s. The elongational tests were performed at 160 °C at Hencky strain rates of 0.03 to 10 s^{-1} up to a maximum Hencky strain of $\varepsilon = 4$. Considering the Rouse relaxation time of the linear PS at 160 °C of $\tau_R = \tau_e Z^2$ with $\tau_e = 0.005$ s and $M_{e,PS} = 15$ kg/mol, resulting in 0.045 s for PS43k and 0.18 s for PS90k, strain hardening of the linear PS should start at Hencky strain rates above 22.2 and 5.5 s^{-1} for PS43k and PS90k, respectively. Thus, strain hardening of the Pom-Pom/linear blends at lower strain rates is exclusively caused by the Pom-Pom fraction. Details of the experimental procedures and the linear viscoelastic characterization of the Pom-Pom/linear blends are given by Hirschberg et al. (2023a). Table 1 summarizes the values of the plateau modulus G_N^0 and the zero-shear viscosity $\eta_0$of the pure components and of the blends. As expected for polystyrene, the plateau modulus is around $G_N^0 \approx 200$ kPa. Smaller values are most probably caused by traces of remaining solvent. Figure 1 shows the mastercurves of G' and G'' for the blend of 20 wt% Pom-Pom PS280k-2x22-22k and 80 wt% of PS star 11-25k, as well as the corresponding plot of the loss tangent δas a function of G'. As in the case of the Pom-Pom/linear blends, we identify the plateau modulus G_N^0 with the value of the storage modulus G' at the high frequency G' minimum of the loss tangent δ. The dynamically diluted backbone chains of the Pom-Pom

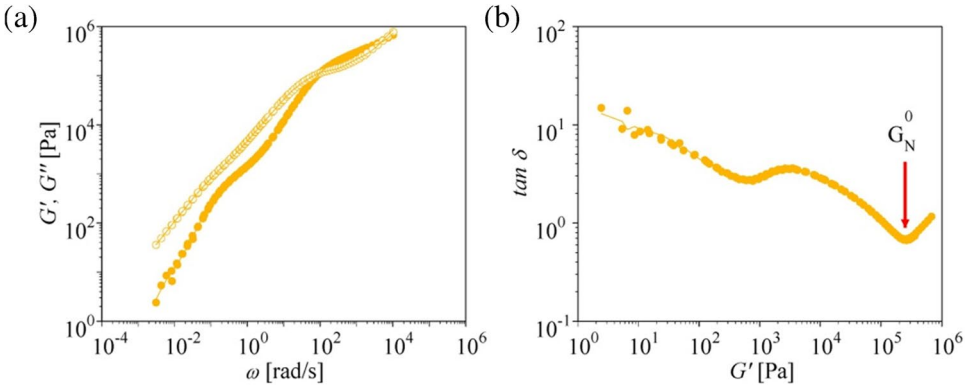

Fig. 1 Experimental data (symbols) of **a** storage (G') and loss (G'') modulus as a function of the angular frequency as well as **b** loss tanδ vs. G' for the blend of 20 wt% Pom-Pom PS280k-2x22-22k and 80 wt% of PS star 11-25k at $T_{ref} = 160$ °C. Lines are fit by parsimonious relaxation spectrum

PS280k-2x22-22k create a shallow minimum at a lower value of G'. The values of G_N^0 and the zero-shear viscosity η_0 of the blend Pom-Pom/star are given in Table 2. The partial moduli g_i and relaxation times τ_i of the parsimonious relaxation spectrum as determined by the IRIS software (Poh et al. 2022; Winter and Mours 2006) are in excellent agreement with the linear viscoelastic data and are summarized in the Support Information (SI) for all blends considered.

Hierarchical Molecular Stress Function (HMMSF) model with enhanced relaxation of stretch (ERS)

We shortly recall the assumptions of the Hierarchical Multimode Molecular Stress Function (HMMSF) model. The extra stress tensor of the HMMSF model is given by:

$$\sigma(t) = \sum_i \int_{-\infty}^{+\infty} \frac{\partial G_i(t-t')}{\partial t'} f_i^2(t,t') S_{DE}^{IA}(t,t') dt' \tag{1}$$

Here $\mathbf{S}_{DE}^{IA}$ is the Doi and Edwards (DE) strain tensor assuming an independent alignment (IA) of tube segments, which is five times the second order orientation tensor $\mathbf{S}$. The molecular stress functions $f_i = f_i(t,t')$ are the inverse of the relative tube diameters a_i of each mode i and are functions of both the observation time t and the time t' of creation of tube segments by reptation. The relaxation modulus $G(t)$ of the melt is represented by discrete Maxwell modes with partial relaxation moduli g_i and relaxation times τ_i:

$$G(t) = \sum_i G_i(t) = \sum_i g_i \exp\left(t/\tau_i\right) \tag{2}$$

The Molecular Stress Function (MSF) model is recovered from Eq. (1) by assuming that the molecular stress functions f_i are identical for all relaxation modes, i.e., $f_i = f$, and f is derived from an energy balance with f^2 being proportional to the stored strain energy in the system, leading to an evolution equation for f with two fitting parameters in extensional flows, β and f_{max} (Wagner et al. 2003). While the parameter β determines the slope of the elongational stress growth coefficient, the maximum possible stretch is represented by the parameter f_{max}, which determines the steady-state elongational viscosity. As shown by Hirschberg et al. (2023a), the elongational viscosity of the Pom-Pom/linear blends with Pom-Pom weight fractions above 10 wt% can be described with reasonable accuracy by a suitable choice of the parameters β and f_{max}.

However, we note that the weight fractions w_i of tube segments of mode i as represented by the partial relaxation moduli g_i of the linear viscoelastic relaxation modulus of Eq. (2) are affected differently by hierarchical relaxation and dynamic dilution, and this can be taken into account by molecular stress functions f_i, which are different for different relaxation modes as explained in the following. For polydisperse polymers, there exist two dilution regimes: the regime of permanent dilution and the regime of dynamic dilution. Permanent dilution occurs due to the presence of oligomeric chains and un-entangled (fluctuating) chain ends. The HMMSF model assumes that the onset of dynamic dilution starts as soon as the relaxation process has reached the dilution modulus $G_D \le G_N^0$. The dilution modulus G_D is a free parameter of the model, which needs to be fitted to nonlinear viscoelastic experimental evidence, since the mass fraction of oligomeric chains and un-entangled chain ends is in general not known a priori. However, for model polymers with well-defined topology such as Pom-Poms, the dilution modulus can be equated with the plateau modulus G_N^0 (Hirschberg et al. 2023b). At time $t = \tau_D$, the relaxation modulus $G(t)$ has relaxed to the value of G_D, and dynamic dilution starts, while at relaxation times $t \le \tau_D$, the chain segments are assumed to be permanently diluted. Hence, the dilution modulus G_D separates the zone of permanent dilution from the zone of dynamic dilution. The weight fraction w_i of dynamically diluted linear or long-chain branched (LCB) polymer segments with relaxation time $\tau_i > \tau_D$ is determined by considering the ratio of the relaxation modulus at time $t = \tau_i$ to the dilution modulus G_D:

$$\begin{aligned} w_i^2 = \frac{G(t=\tau_i)}{G_D} = \frac{1}{G_D}\sum_{j=1}^{n} g_j \exp\left(-\tau_i/\tau_j\right) \quad & \text{for } \tau_i > \tau_D \\ w_i^2 = 1 \quad & \text{for } \tau_i \le \tau_D \end{aligned} \tag{3}$$

The value of w_i obtained at $t = \tau_i$ is attributed to the chain segments with relaxation time τ_i. Segments with $\tau_i < \tau_D$ are considered to be permanently diluted, i.e., their weight fractions are fixed at $w_i = 1$. As shown by Narimissa et al. (2015), these assumptions allow modeling the rheology of broadly distributed polymers, largely independent of the number of discrete Maxwell modes used to represent the relaxation modulus $G(t)$.

Restricting attention to LCB polymers and extensional flows, the evolution equation for the molecular stress function f_i of each mode i was originally expressed by Narimissa et al. (2015) as:

$$\frac{\partial f_i}{\partial t} = f_i(K : S) - \frac{1}{3}\frac{f_i - 1}{\tau_i}\left(1 - \frac{2}{3}w_i^2\right) - \frac{2}{3}\frac{f_i^2\left(f_i^3 - 1\right)}{3\tau_i}w_i^2 \tag{4}$$

with the initial conditions $f_i(t = t',t') = 1$. The first term on the right-hand side represents the affine stretch rate with $\mathbf{K}$ the velocity gradient tensor, the second term takes into account stretch relaxation in the longitudinal direction of the tube, and the third term limits molecular stretch due to the interchain

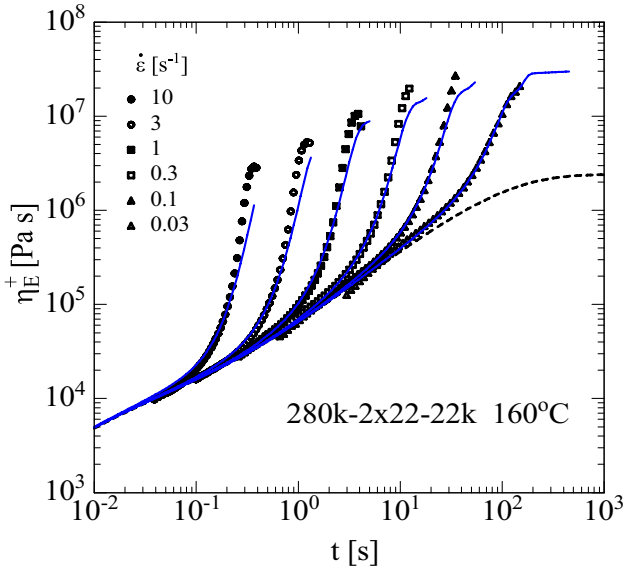

Fig. 2 Experimental data (symbols) of elongational stress growth coefficient $\eta_E^+(t)$ as a function of time t for the pure Pom-Pom 280k-2x22-22k at $T = 160$ °C. Lines are predictions of the HMMSF model; dotted line is LVE start-up viscosity

tube pressure in the lateral direction of a tube segment. The effect of dynamic dilution enters Eq. (4) via the square of the weight fractions w_i and takes into account that the effect of dynamic dilution vanishes in fast flows. It may be surprising at first that the stretch relaxation times in Eq. (4) can be equated with the relaxation times τ_i. However, we note that in the case of the highly branched Pom-Pom considered here as well as in Hirschberg et al. (2023b), the backbone chain is firmly embedded into the deforming polymer environment by the two branch points with multiple arms. Therefore, stretch relaxation cannot occur by Rouse relaxation along the confining tube of the backbone, nor by branch point withdrawal of the arms into the tube as in the case of H-shaped polymers or randomly branched polyethylene melts leading to elongational viscosity overshoots (Wagner et al. 2022). Rather, the Pom-Pom systems fail by brittle fracture at higher strain and strain rates as shown by Hirschberg et al. (2023b). Stretch relaxation of these Pom-Poms with multiple arms can only occur by constraint release processes along the backbone chain. In the case of entangled backbones, constraints of the test chain by other backbone chains are released by dynamic dilution–assisted reptation, while in the case of un-entangled backbones, Rouse relaxation is constrained by the presence of the Pom-Pom

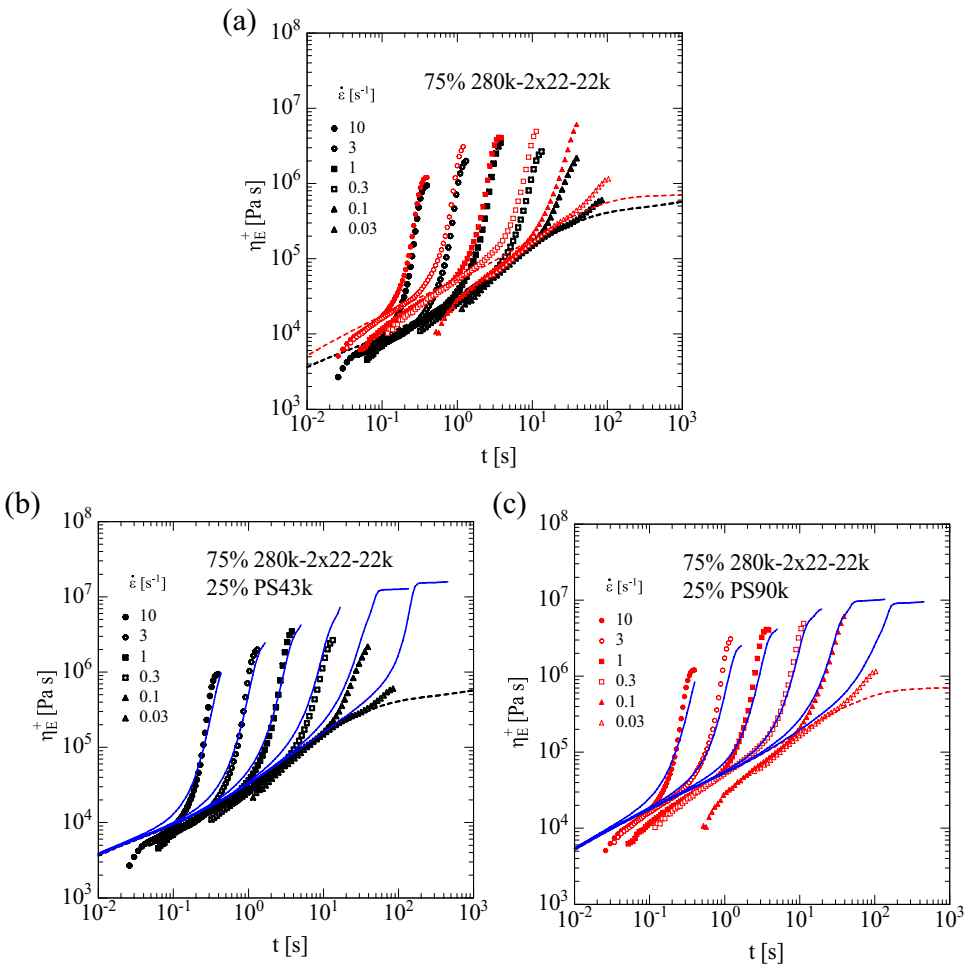

Fig. 3 **a–c** Experimental data of elongational stress growth coefficient $\eta_E^+(t)$ as a function of time t for blends of 75 wt% Pom-Pom 280k-2x22-22k and 25 wt% PS43k (black symbols) and PS90k (red symbols), respectively. Lines are predictions of the HMMSF model; dotted lines are LVE start-up viscosity

arms and in the case of Pom-Pom/linear blends, in addition by the presence of the linear PS blend component. In both cases, the relevant stretch relaxation times are the relaxation times τ_i representing the escape times of backbone chain segments due to constraint release. As long as a backbone chain segment characterized by τ_i is confined by a tube segment, it will be oriented and stretched by the flow, and the relevant time scale of stretch relaxation is its relaxation time τ_i. Of course, this argument is only valid for relaxation times which are associated with the relaxation of the backbone chain.

Instead of the interchain pressure term in Eq. (4), which was also used in the analysis of the elongational viscosity of 10 polystyrene Pom-Pom melts by Hirschberg et al. (2023b), we generalize here the enhanced relaxation of stretch (ERS) concept of Wagner and Narimissa (2021): when considering a control volume of diameter and length a_i representing the decreasing diameter of a tube segment with increasing deformation, the number of monomers in this control volume decreases with deformation with the consequence of enhanced relaxation of stretch on smaller length scales, leading to a stretch relaxation term which is proportional to the 5th power of the stretch f_i. The evolution equation is then given as:

$$\frac{\partial f_i}{\partial t} = f_i(K:S) - \frac{f_i - 1}{\tau_i}\left(1 - w_i^2\right) - \frac{\left(f_i^5 - 1\right)}{5\tau_i} w_i^2 \tag{5}$$

As seen by comparing Eqs. (4) and (5), the ERS concept leads to a simplified structure of the evolution equation for the stretch, while the leading 5th power of stretch relaxation is the same in both equations. The effect of dynamic dilution on the stress becomes clearly evident when considering the limit of fast flows. For fast elongational flow with Weissenberg numbers $Wi_i = \dot{\varepsilon}\tau_i$, the elongational stress in the limit of high strain, when $\partial f_i/\partial t = 0$, is obtained from Eqs. (1) and (5) as:

$$\sigma_E = 5\sum_i g_i f_i^2 = 5\sum_i g_i \frac{\sqrt{5Wi_i}}{w_i} = 5\sum_i g_{i0} w_i \sqrt{5Wi_i} \tag{6}$$

Here, $g_{i0} = g_i w_i^{-2}$is the undiluted partial relaxation modulus (assuming a dilution exponent of *1*), and the contribution of the relaxation mode *i* to the elongational stress

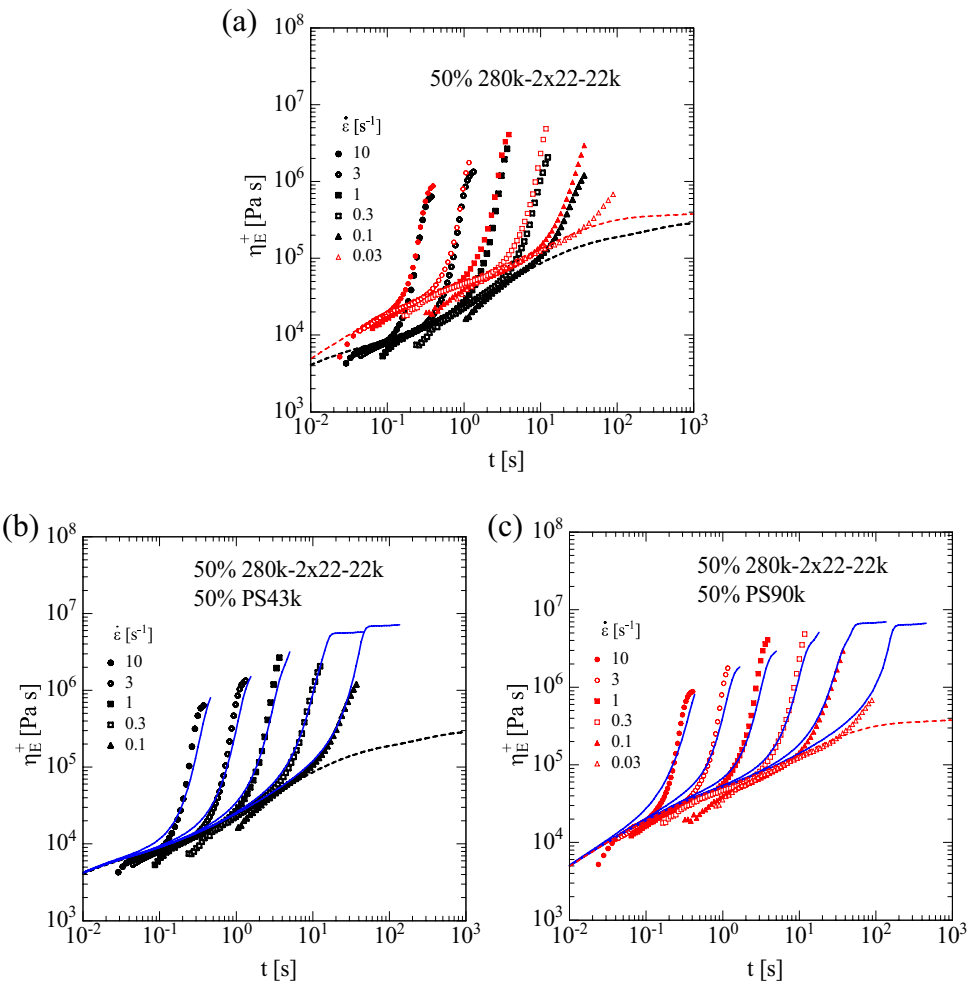

Fig. 4 **a–c** Experimental data of elongational stress growth coefficient $\eta_E^+(t)$ as a function of time *t* for blends of 50 wt% Pom-Pom 280k-2x22-22k and 50 wt% PS43k (black symbols) and PS90k (red symbols), respectively. Lines are predictions of the HMMSF model; dotted lines are LVE start-up viscosity

is proportional to the weight fraction of the undiluted partial relaxation modulus g_{i0}.

Thus, the HMMSF model for polydisperse polymer melts consists of the multi-mode stress equation (Eq. 1), a set of evolution equations for the molecular stresses f_i, Eq. (5), and a hierarchical procedure to quantify the fraction of dynamically diluted chain segments according to Eq. (3) with only one free nonlinear parameter, the dilution modulus G_D. Once the linear viscoelastic relaxation spectrum of a polydisperse polymer melt is known, the weight fractions w_i in the evolution Eq. (5) can be obtained by fitting the value of G_D to the elongational viscosity. The parameter G_D, in conjunction with the relaxation times τ_i, determines the extent of strain hardening. This one free parameter is sufficient for modeling extensional flows. As we will show below, for the Pom-Pom and the blends of Pom-Pom/linear and Pom-Pom/star considered here, the dilution modulus G_D is equivalent to the plateau modulusG_N^0; i.e., dynamic dilution starts as soon as the relaxation modulus $G(t)$ of Eq. (3) reaches G_N^0 and the hierarchical relaxation of the arms of the Pom-Pom increases the tube diameter of the backbone chain segments.

To model the fracture of polymer melts, we use the fracture criterion of Wagner et al. (2022) and assume that fracture occurs as soon as the entanglement segments correspond to one relaxation mode i fracture, i.e., when these segments reach the critical value W_c of the strain energy:

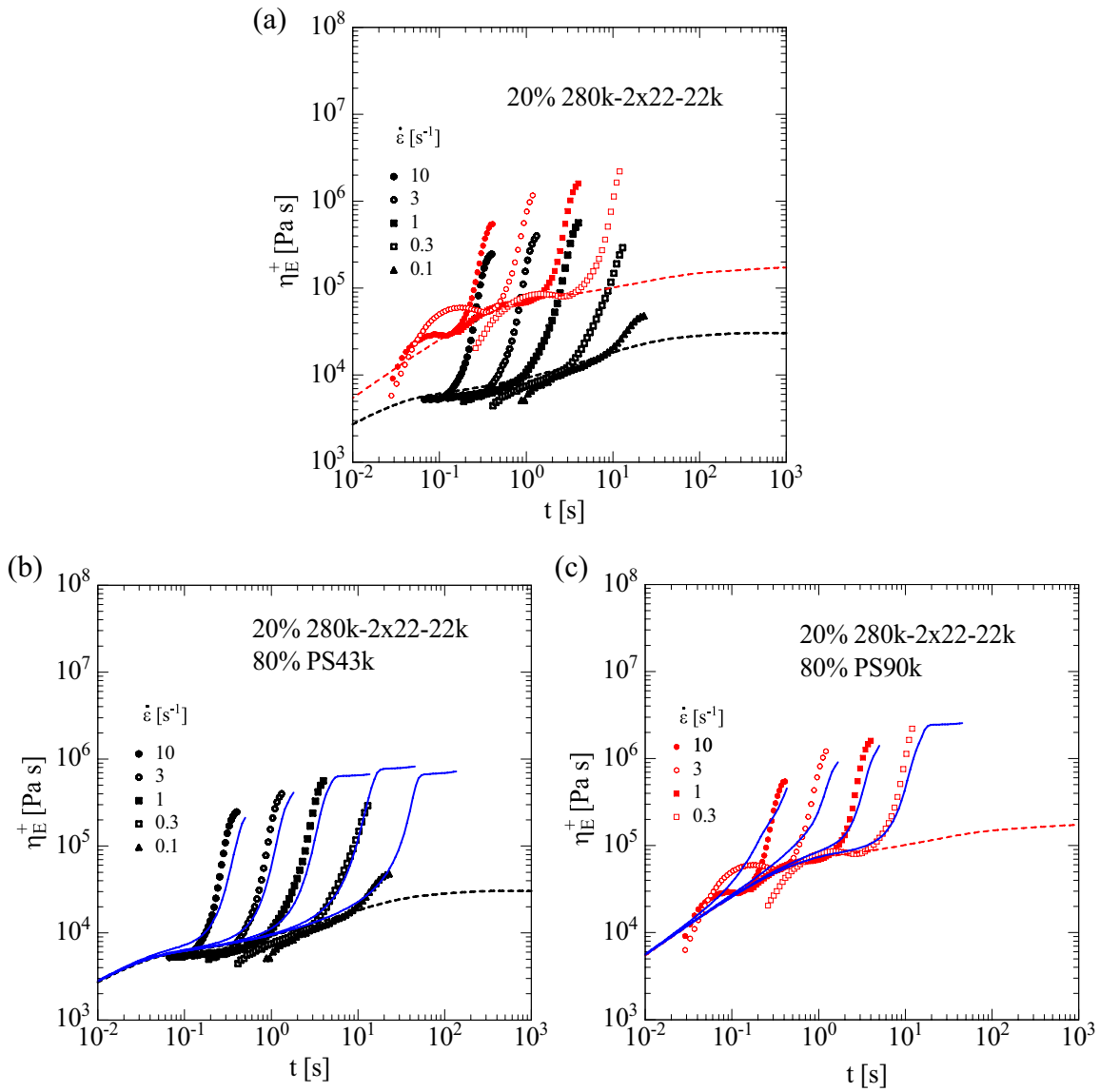

Fig. 5 **a–c** Experimental data of elongational stress growth coefficient $\eta_E^+(t)$ as a function of time t for blends of 20 wt% Pom-Pom 280k-2x22-22k and 80 wt% PS43k (black symbols) and PS90k (red symbols), respectively. Lines are predictions of the HMMSF model; dotted lines are LVE start-up viscosity

$$W_c = 3kTf_{i,c}^2 w_i = U \tag{7}$$

U is the bond-dissociation energy of a single carbon-carbon bond in hydrocarbons. The strain energy of a diluted chain segment is given by $W = 3kTf_i w_i$ with f_i obtained from Eq. (5), and the ratio of bond-dissociation energy U (ca. 3–4 eV, 350 kJ/mol) to thermal energy $3kT$ is approximately $U/3kT = 32$ at a temperature of $T = 160$ °C. According to the entropic fracture hypothesis, when the strain energy of the entanglement segment reaches the critical energy U, the total strain energy of the chain segment will be concentrated on *one* C-C bond by thermal fluctuations, and this bond will rupture. This leads to crack initiation and within a few milliseconds to brittle fracture of the sample, as shown for binary PS blends (Wagner et al. 2021) as well as for low-density polyethylene melts (Poh et al. 2023). Equation (7) defines the square of the critical stretch $f_{i,c}$ at fracture:

$$f_{i,c}^2 = \frac{U}{3kT}\frac{1}{w_i} \tag{8}$$

For the polymers investigated here, fracture is at first triggered by the mode with the longest relaxation time, followed at higher strain rates by fracture of shorter relaxation modes.

Modeling elongational viscosity data of Pom-Pom/linear blends

Figure 2 compares the experimental data (symbols) of the elongational stress growth coefficient $\eta_E^+(t)$ as a function of time t for the pure Pom-Pom 280k-2x22-22k at $T = 160$ °C as reported by Hirschberg et al. (2023b) to predictions (lines) of the HMMSF model. The Pom-Pom melt shows strong strain hardening, i.e., the maximal elongational viscosities η_E measured are much larger than the linear viscoelastic start-up viscosity η_E^0 at the corresponding Hencky strain, and the strain hardening factor defined by η_E/η_E^0 reaches values of SHF ≈ 100. The elongational stress growth coefficient of the Pom-Pom melt is well described by the HMMSF model within experimental accuracy, based exclusively on the linear viscoelastic relaxation spectra as input and without the

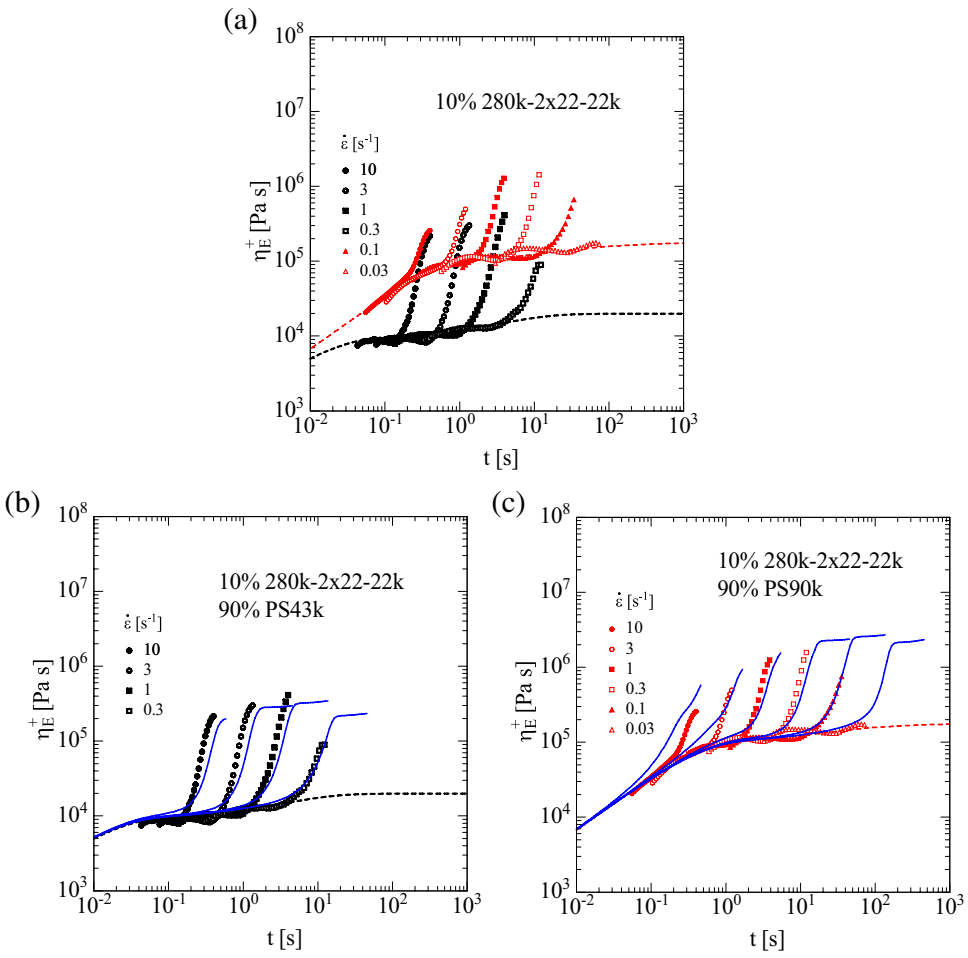

Fig. 6 **a–c** Experimental data of elongational stress growth coefficient $\eta_E^+(t)$ as a function of time t for blends of 10 wt% Pom-Pom 280k-2x22-22k and 90 wt% PS43k (black symbols) and PS90k (red symbols), respectively. Lines are predictions of the HMMSF model; dotted lines are LVE start-up viscosity

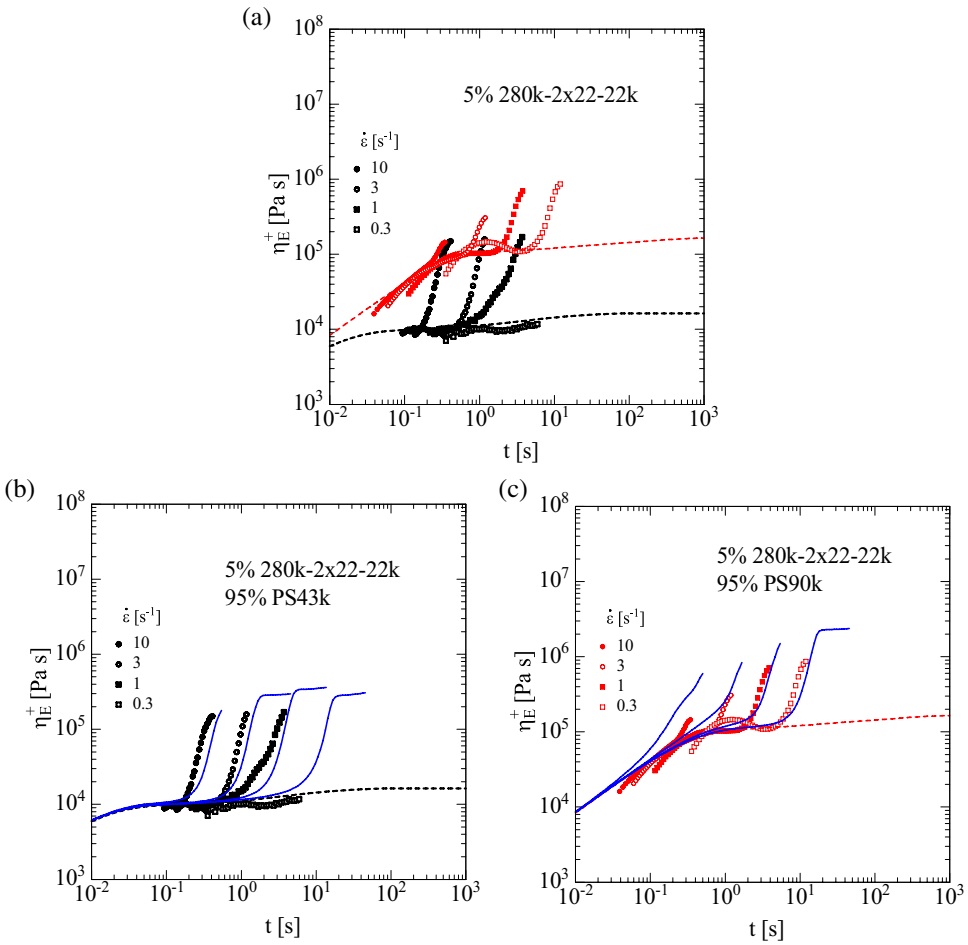

Fig. 7 **a**–**c** Experimental data of elongational stress growth coefficient $\eta_E^+(t)$ as a function of time t for blends of 5 wt% Pom-Pom 280k-2x22-22k and 95 wt% PS43k (black symbols) and PS90k (red symbols), respectively. Lines are predictions of the HMMSF model; dotted lines are LVE start-up viscosity

use of any further model parameter. We note that in contrast to Hirschberg et al. (2023b), we use evolution Eq. (5) here instead of Eq. (4). However, predictions agree within line width of the curve of the model visibly with the results reported earlier for Pom-Pom 280k-2x22-22k. Except for the lowest strain rate, the entropic fracture criterion of Eq. (8) predicts fracture of the samples at Hencky strains of $\varepsilon \cong 4$ or larger. While this is in agreement with the fact that the samples can be stretched up to the experimental limit of $\varepsilon = 4$, no definite statement about the validity of the fracture criterion can be made here, but we note that within experimental accuracy, the entropic fracture criterion was shown to describe the occurrence of brittle fracture quantitatively for the Pom-Pom systems investigated by Hirschberg et al. (2023b) over a wide range of elongation rates from 0.004 to 210 s^{-1}.

Figures 3, 4, 5, 6, 7, and 8 present the elongational viscosity data at T = 160 °C and their comparison to the HMMSF model for the blends with 75, 50, 20, 10, 5, and 2 wt% of Pom-Pom 280k-2x22-22k and the corresponding weight fractions of PS43k (black symbols) and PS90k (red symbols), respectively. This allows a direct comparison of the effect of the two diluents on the strain hardening behavior. For the blends with 75 and 50 wt% of Pom-Pom (Figs. 3a and 4a), the elongational stress growth coefficient $\eta_E^+(t)$of the blends is very similar irrespective whether blended with PS43k or PS90k. The zero-elongational viscosity of these blends is mainly dominated by the viscosity of the Pom-Pom. This does change increasingly for blends with lower concentration of the Pom-Pom (Figs. 5a, 6, 7, and 8a), when the higher zero-shear viscosity of PS90k compared to PS43k becomes apparent. For the case of 20 wt% of Pom-Pom 280k-2x22-22k, the elongational stress growth coefficient $\eta_E^+(t)$of the blend with PS43k (black symbols in Fig. 5a) is clearly lower than for the blend with PS90k (red symbols in Fig. 5a). For blends with Pom-Pom 280k-2x22-22k concentrations of 10 wt% or lower (Figs. 6a, 7, and 8a), it is interesting to note that at the highest strain rate of 10 s^{-1}, the maximal values of the elongational stress growth coefficient $\eta_E^+(t)$ are largely independent of the type of the matrix, PS43k or PS90k, while at lower strain rates, the blends with PS90k show significantly higher elongational viscosities in line with the higher LVE start-up viscosity of PS90k. This agrees with earlier results on the elongational viscosity

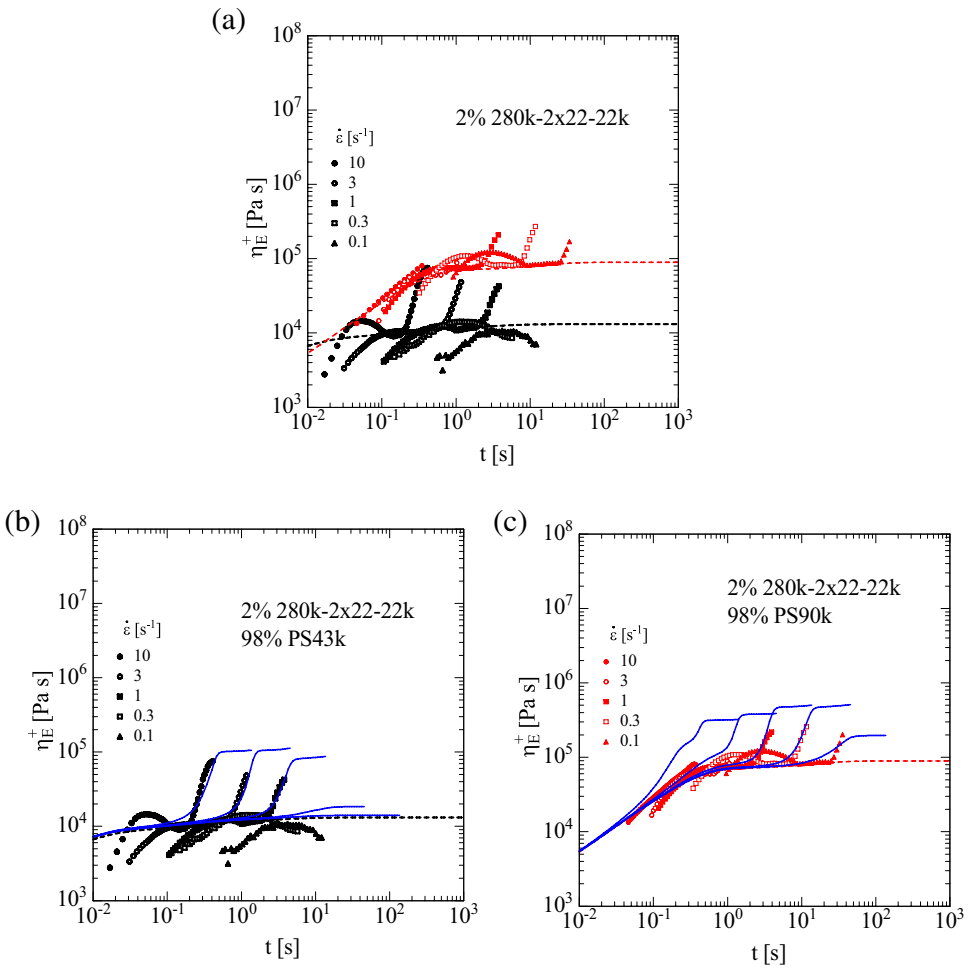

Fig. 8 **a–c** Experimental data of elongational stress growth coefficient $\eta_E^+(t)$ as a function of time t for blends of 2 wt% Pom-Pom 280k-2x22-22k and 98 wt% PS43k (black symbols) and PS90k (red symbols), respectively. Lines are predictions of the HMMSF model; dotted lines are LVE start-up viscosity

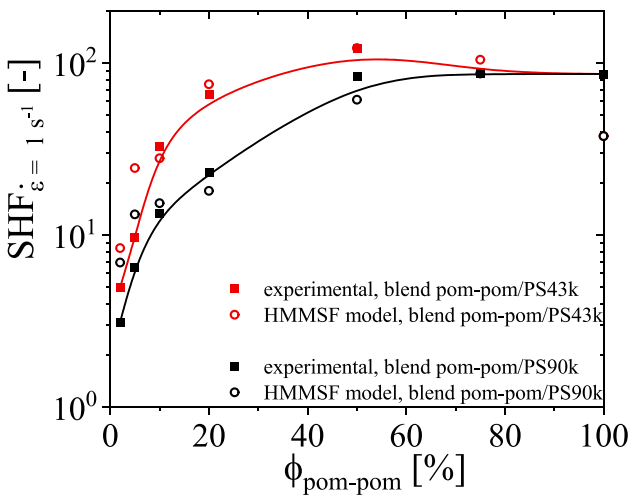

Fig. 9 Comparison of the SHF at $\dot{\varepsilon} = 1\ s^{-1}$ from experimental data and the prediction via the HMMSF model for the blends of Pom-Pom 280k-2x22-22k with PS43k (red) and PS90k (black). The red and black lines are guides for the eye for the experimental data

of bidisperse blends consisting of a high and several low molar mass linear polystyrenes reported by Wagner et al. (2021), who showed that the stretching of the long chains is widely independent of the molar mass of the matrix reaching from non-entangled oligomeric styrene (8.8 kg/mol) to well-entangled polystyrene (73 kg/mol). As shown in Figs. 3, 4, 5, 6, 7, and 8, the elongational flow data the Pom-Pom/linear blends are well described by the HMMSF model within experimental accuracy, irrespective of the concentration of Pom-Pom 280k-2x22-22k and irrespective of the linear blend component, PS43k or PS90k. This is achieved solely by the use of the LVE characterization of the blends, i.e., linear viscoelastic relaxation spectrum and plateau modulus, as input and without the need for any further model parameter. Only for the Pom-Pom 280k-2x22-22k/PS90k blends with Pom-Pom concentrations of 10% or lower and strain rates of 3 and 10 s^{-1}, the maximal values of the elongational viscosity predicted by the HMMSF model are higher than

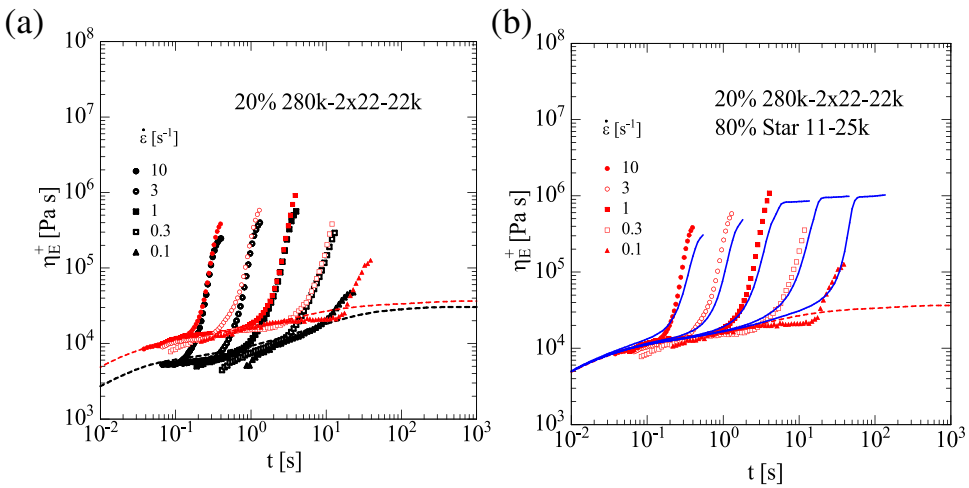

Fig. 10 **a–b** Experimental data of elongational stress growth coefficient $\eta_E^+(t)$ as a function of time t for blends of 20% Pom-Pom 280k-2x22-22k and 80% PS43k (black symbols) and PS star 11-25k (red symbols), respectively. Lines are predictions of the HMMSF model; dotted lines are LVE start-up viscosity

observed experimentally. Besides experimental issues as seen in Figs. 7 and 8, this may be due to the fact that at these low concentrations of Pom-Pom 280k-2x22-22k, the relevant relaxation times for stretch of the Pom-Pom fraction are convoluted with the relaxation times of PS90k, and the limit of the validity of the assumptions leading to the stretch evolution equation (Eq. 5) of the HMMSF model may have been reached. In agreement with the experimental data, which are limited to Hencky strains of $\varepsilon \leq 4$, the entropic fracture criterion of Eq. (8) predicts fracture of the samples at Hencky strains of $\varepsilon \cong 4$ or larger at the higher strain rates investigated, while at lower strain rates, the approach to a steady-state elongational viscosity is predicted.

To quantitatively compare predictions of the HMMSF model and experimental data, the maximal experimental and modeled values of the strain hardening factor (SHF) at $\dot{\varepsilon} = 1\ s^{-1}$ are plotted in Fig. 9 as a function of the Pom-Pom weight fraction Φ. The SHF is the ratio between the maximal elongational viscosity and the value of the elongational viscosity obtained by the Doi-Edwards equation, i.e., by considering only orientation and no stretching of polymer chains (Hirschberg et al. 2023a). The comparison reveals for the blends above 10 wt% Pom-Pom deviations of less than 25% between the measured and the predicted SHF. This represents an excellent agreement within experimental accuracy, considering that the HMMSF model uses only the SAOS mastercurve as input. For 2 and 5 wt% Pom-Pom, the deviation of the predicted SHF from the experimental value becomes larger, and the HMMSF model overestimates the measured SHF. As discussed in Hirschberg et al. (2023a), the experimental error at low Pom-Pom contents increases, as the zero-shear viscosity of the blends decreases, but Figs. 7 and 8 still show excellent agreement of experimental and modeled elongational stress growth coefficient $\eta_E^+(t)$with much lower deviations of the SHF for individual strain rates.

Modeling elongational viscosity of Pom-Pom/star blend

Figure 10a compares the measurements of the elongational stress growth coefficient $\eta_E^+(t)$ for the blend of 20 wt% Pom-Pom 280k-2x22-22k and 80 wt% PS star 11-25k (red symbols) with data of the blend of 20 wt% Pom-Pom 280k-2x22-22k and 80 wt% linear PS43k (black symbols) at $T = 160$ °C. The direct comparison reveals the surprising fact that the blend Pom-Pom/star and the blend Pom-Pom/linear show nearly the same strain hardening in elongational flow. Although the star with 11 arms of $M_{w,a} = 25$ kg/mol has a molecular weight of $M_w = 275$ kg/mol which corresponds to the molecular weight of the backbone of the Pom-Pom, it has only a slightly higher zero-shear viscosity as the linear PS43k (5.1 kPas vs. 3.0 kPas) as given in Tables 1 and 2. However, it has a similar span molecular weight as PS43k, which determines not only the zero-shear viscosity of the star but also the Rouse time which is expected to be of the same order of magnitude as for the linear PS43k. Thus, the star by itself does not show strain hardening in the experimental window of the strain rates investigated and therefore does not contribute to the strain hardening. This is alike the vanishing strain hardening of the linear Polystyrene at 43 kg/mol. Consequently, the strain hardening is solely due to the Pom-Pom polymer. Predictions (lines) of the HMMSF model are compared to the elongational stress growth coefficient $\eta_E^+(t)$of the blend

of 20 wt% Pom-Pom 280k-2x22-22k and 80 wt% PS star 11-25k in Fig.10b, and good agreement is found within experimental accuracy.

Conclusions

The Hierarchical Multi-mode Molecular Stress Function (HMMSF) model is based on the assumption that the linear viscoelastic spectrum of relaxation of polymer melts already incorporates the rheological effect of polydispersity. In the case of LCB polymers, the linear viscoelastic relaxation spectrum also contains the effect of the often-unknown molecular branching topology. Therefore, only a few specific constitutive assumptions concerning the prediction of the nonlinear rheology are needed, thereby reducing the number of adjustable free nonlinear material parameters to an absolute minimum. The original HMMSF model was based on the linear viscoelastic relaxation modulus and the basic concepts of hierarchical relaxation, dynamic dilution, and interchain tube pressure. In this contribution, we have replaced the interchain tube pressure concept by the enhanced relaxation of stretch (ERS) model, which is based on the idea of enhanced stretch relaxation at smaller length scales. A decreasing tube diameter with increasing deformation leads to faster relaxation of stretch, which sets a limit on the minimum tube segment diameter and thereby the maximum stretch of the chain segment for a given deformation rate. Thus, the ERS concept has a more fundamental basis than the original interchain tube pressure idea relying on a tube diameter relaxation time (Narimissa et al. 2015). Through hierarchical relaxation, dynamic dilution results in larger tube diameters of chain segments at equilibrium. Dynamic dilution starts when the relaxation modulus $G(t)$ reaches the dilution modulus G_D. In nonlinear flow, the "dynamic" part of dilution (as quantified by the dilution modulus G_D) decreases with increasing strain rate. For the Pom-Pom and the Pom-Pom blends considered here, the dilution modulus G_D is equivalent to the plateau modulusG_N^0; i.e., dynamic dilution starts as soon as the relaxation modulus $G(t)$ reaches G_N^0 and the hierarchical relaxation of the arms of the Pom-Pom increase the tube diameter of the backbone chain segments. This is independent of whether the neat Pom-Pom or its blends with linear or star PS are considered, provided the linear or star blend components do not show strain hardening on their own. The HMMSF model is found to be in agreement with the elongational viscosity data of the Pom-Pom and the Pom-Pom blends, using only the linear viscoelastic relaxation spectrum and the plateau modulus as input. To the knowledge of the authors, this has not been achieved by any other constitutive equation so far. The result is of importance not only with respect to the understanding of the interaction of Pom-Pom topologies with linear or even star-shaped diluents in elongational flow but also for the tailoring of blends with optimal balance of strain hardening and viscosity for polymer processing. Neat Pom-Pom systems with long backbones and many arms show not only strong strain hardening but also a very high zero-shear viscosity, while blending of 2–10 wt% of the same Pom-Pom into a lower molecular weight linear polymer reduces the viscosity by 2 orders of magnitude while still preserving a strong strain hardening. Furthermore, it paves the way to tune rheological properties of, e.g., recycled polymers with unknown properties with the addition of small amounts of well-designed branched polymers.

Supplementary Information The online version contains supplementary material available at https://doi.org/10.1007/s00397-023-01411-1.

Acknowledgements The authors thank Dr. Michael Pollard for proof reading of the manuscript as a native English speaker.

Funding Open Access funding enabled and organized by Projekt DEAL.

Declarations

Conflict of interest The authors declare no competing interests.

References

Abbasi M, Faust L, Riazi K, Wilhelm M (2017) Linear and extensional rheology of model branched polystyrenes: from loosely grafted combs to bottlebrushes. Macromolecules 50:5964–5977. https://doi.org/10.1021/acs.macromol.7b01034

Ahirwal D, Filipe S, Neuhaus I, Busch M, Schlatter G, Wilhelm M (2014) Large amplitude oscillatory shear and uniaxial extensional rheology of blends from linear and long-chain branched polyethylene and polypropylene. J Rheol 58:635–658. https://doi.org/10.1122/1.4867555

Ajji A, Sammut P, Huneault MA (2003) Elongational rheology of LLDPE/LDPE blends. J Appl Polym Sci 88:3070–3077. https://doi.org/10.1002/app.11931

Ebrahimi T, Taghipour H, Grießl D, Mehrkhodavandi P, Hatzikiriakos SG, van Ruymbeke E (2017) Binary blends of entangled star and linear poly(hydroxybutyrate): effect of constraint release and dynamic tube dilation. Macromolecules 50:2535–2546. https://doi.org/10.1021/acs.macromol.6b02653

Hirschberg V, Lyu S, Schußmann MG (2023a) Complex polymer topologies in blends: shear and elongational rheology of linear/pom-pom polystyrene blends. J Rheol 67:403–415. https://doi.org/10.1122/8.0000544

Hirschberg V, Schußmann MG, Röpert MC, Wilhelm M, Wagner MH (2023b) Modeling elongational viscosity and brittle fracture of

10 polystyrene Pom-Poms by the hierarchical molecular stress function model. Rheol Acta 62:269–283. https://doi.org/10.1007/s00397-023-01393-0

Huang Q (2022) When polymer chains are highly aligned: a perspective on extensional rheology. Macromolecules 55:715–727. https://doi.org/10.1021/acs.macromol.1c02262

Ianniello V, Costanzo S (2022) Linear and nonlinear shear rheology of nearly unentangled H-polymer melts and solutions. Rheol Acta 61:667–679. https://doi.org/10.1007/s00397-022-01349-w

Larson RG (1999) The structure and rheology of complex fluids. Oxford University Press, New York [etc.]

Larson RG (2001) Combinatorial rheology of branched polymer melts. Macromolecules 34:4556–4571. https://doi.org/10.1021/ma000700o

Lentzakis H, Costanzo S, Vlassopoulos D, Colby RH, Read DJ, Lee H, Chang T, van Ruymbeke E (2019) Constraint release mechanisms for H-polymers moving in linear matrices of varying molar masses. Macromolecules 52:3010–3028. https://doi.org/10.1021/acs.macromol.9b00251

Lentzakis H, Vlassopoulos D, Read DJ, Lee H, Chang T, Driva P, Hadjichristidis N (2013) Uniaxial extensional rheology of well-characterized comb polymers. J Rheol 57:605. https://doi.org/10.1122/1.4789443

López-Barrón CR, Zeng Y, Richards JJ (2017) Chain stretching and recoiling during startup and cessation of extensional flow of bidisperse polystyrene blends. J Rheol 61:697. https://doi.org/10.1122/1.4983828

McKinley GH, Hassager O (1999) The Considère condition and rapid stretching of linear and branched polymer melts. J Rheol 43:1195–1212. https://doi.org/10.1122/1.551034

McLeish TCB, Allgaier J, Bick DK, Bishko G, Biswas P, Blackwell R, Blottière B, Clarke N, Gibbs B, Groves DJ, Hakiki A, Heenan RK, Johnson JM, Kant R, Read DJ, Young RN (1999) Dynamics of entangled H-polymers: theory, rheology, and neutron-scattering. Macromolecules 32:6734–6758. https://doi.org/10.1021/ma990323j

McLeish TCB, Larson RG (1998) Molecular constitutive equations for a class of branched polymers: the pom-pom polymer. J Rheol 42:81–110. https://doi.org/10.1122/1.550933

Narimissa E, Rolon-Garrido VH, Wagner MH (2015) A hierarchical multi-mode MSF model for long-chain branched polymer melts part I: elongational flow. Rheol Acta 54:779–791

Nielsen JK, Rasmussen HK, Hassager O, McKinley G (2006) Elongational viscosity of monodisperse and bidisperse polystyrene melts. J Rheol 50:453. https://doi.org/10.1122/1.2206711

Poh L, Narimissa E, Wagner MH, Winter HH (2022) Interactive shear and extensional rheology—25 years of IRIS Software. Rheol Acta 61:259–269. https://doi.org/10.1007/s00397-022-01331-6

Poh L, Wu Q, Pan Z, Wagner MH, Narimissa E (2023) Fracture in elongational flow of two low-density polyethylene melts. Rheol Acta 62:317–331. https://doi.org/10.1007/s00397-023-01392-1

Röpert M-C, Goecke A, Wilhelm M, Hirschberg V (2022b) Threading polystyrene stars: impact of star to pom-pom and barbwire topology on melt rheological and foaming properties. Macromol Chem Phys 223:2200288. https://doi.org/10.1002/macp.202200288

Röpert M-C, Schußmann MG, Esfahani MK, Wilhelm M, Hirschberg V (2022a) Effect of side chain length in polystyrene pom–poms on melt rheology and solid mechanical fatigue. Macromolecules 55:5485–5496. https://doi.org/10.1021/acs.macromol.2c00199

Shahid T, Clasen C, Oosterlinck F, van Ruymbeke E (2019) Diluting entangled polymers affects transient hardening but not their steady elongational viscosity. Macromolecules 52:2521–2530. https://doi.org/10.1021/acs.macromol.8b02701

Stange J, Uhl C, Münstedt H (2005) Rheological behavior of blends from a linear and a long-chain branched polypropylene. J Rheol 49:1059–1079. https://doi.org/10.1122/1.2008297

Szántó L, Feng Y, Friedrich C (2021) Extensional hardening of multimodal, linear PE with high amounts of UHMWPE. J Rheol 65:371–380. https://doi.org/10.1122/8.0000197

Tan L, Pan J, Wan A (2012) Shear and extensional rheology of polyacrylonitrile solution: effect of ultrahigh molecular weight polyacrylonitrile. Colloid Polym Sci 290:289–295. https://doi.org/10.1007/s00396-011-2546-1

Wagner MH, Kheirandish S, Koyama K, Nishioka A, Minegishi A, Takahashi T (2005) Modeling strain hardening of polydisperse polystyrene melts by molecular stress function theory. Rheol Acta 44:235–243. https://doi.org/10.1007/s00397-004-0402-7

Wagner MH, Kheirandish S, Stange J, Münstedt H (2006) Modeling elongational viscosity of blends of linear and long-chain branched polypropylenes. Rheol Acta 46:211–221. https://doi.org/10.1007/s00397-006-0108-0

Wagner MH, Kheirandish S, Yamaguchi M (2004) Quantitative analysis of melt elongational behavior of LLDPE/LDPE blends. Rheol Acta 44:198–218. https://doi.org/10.1007/s00397-004-0400-9

Wagner MH, Narimissa E (2021) A new perspective on monomeric friction reduction in fast elongational flows of polystyrene melts and solutions. J Rheol 65:1413–1421

Wagner MH, Narimissa E, Poh L, Huang Q (2022) Modelling elongational viscosity overshoot and brittle fracture of low-density polyethylene melts. Rheol Acta 61:281–298. https://doi.org/10.1007/s00397-022-01328-1

Wagner MH, Narimissa E, Shahid T (2021) Elongational viscosity and brittle fracture of bidisperse blends of a high and several low molar mass polystyrenes. Rheol Acta 60:803–817. https://doi.org/10.1007/s00397-021-01304-1

Wagner MH, Rolón-Garrido VH, Nielsen JK, Rasmussen HK, Hassager O (2008) A constitutive analysis of transient and steady-state elongational viscosities of bidisperse polystyrene blends. J Rheol 52:67. https://doi.org/10.1122/1.2807442

Wagner MH, Yamaguchi M, Takahashi M (2003) Quantitative assessment of strain hardening of low-density polyethylene melts by the molecular stress function model. J Rheol. https://doi.org/10.1122/1.1562155

Winter HH, Mours M (2006) The cyber infrastructure initiative for rheology. Rheol Acta 45:331–338. https://doi.org/10.1007/s00397-005-0041-7